Environmental Science and Ecotechnology 21 (2024) 100417

Contents lists available at ScienceDirect

Environmental Science and Ecotechnology

journal homepage: www.journals.elsevier.com/environmental-science-and-ecotechnology/

Review

Nonmetallic modified zero-valent iron for remediating halogenated organic compounds and heavy metals: A comprehensive review

Zimin Yan [a], Jia Ouyang [a], Bin Wu [a], Chenchen Liu [a], Hongcheng Wang [b], Aijie Wang [b], Zhiling Li [a, *]

[a] State Key Laboratory of Urban Water Resource and Environment, School of Environment, Harbin Institute of Technology, Harbin, 150090, PR China
[b] State Key Laboratory of Urban Water Resource and Environment, School of Civil and Environmental Engineering, Harbin Institute of Technology Shenzhen, Shenzhen, 518055, PR China

ARTICLE INFO

Article history:
Received 6 October 2023
Received in revised form
15 March 2024
Accepted 16 March 2024

Keywords:
Nonmetallic modified zero-valent iron
Halogenated organic compounds
Heavy metals
Reductive removal
Regulation strategies
Electron selectivity

ABSTRACT

Zero-valent iron (ZVI), an ideal reductant treating persistent pollutants, is hampered by issues like corrosion, passivation, and suboptimal utilization. Recent advancements in nonmetallic modified ZVI (NM-ZVI) show promising potential in circumventing these challenges by modifying ZVI's surface and internal physicochemical properties. Despite its promise, a thorough synthesis of research advancements in this domain remains elusive. Here we review the innovative methodologies, regulatory principles, and reduction-centric mechanisms underpinning NM-ZVI's effectiveness against two prevalent persistent pollutants: halogenated organic compounds and heavy metals. We start by evaluating different nonmetallic modification techniques, such as liquid-phase reduction, mechanical ball milling, and pyrolysis, and their respective advantages. The discussion progresses towards a critical analysis of current strategies and mechanisms used for NM-ZVI to enhance its reactivity, electron selectivity, and electron utilization efficiency. This is achieved by optimizing the elemental compositions, content ratios, lattice constants, hydrophobicity, and conductivity. Furthermore, we propose novel approaches for augmenting NM-ZVI's capability to address complex pollution challenges. This review highlights NM-ZVI's potential as an alternative to remediate water environments contaminated with halogenated organic compounds or heavy metals, contributing to the broader discourse on green remediation technologies.

1. Introduction

Halogenated organic compounds (HOCs) and heavy metals (HMs) are two typical kinds of persistent pollutants that widely exist in aquatic environments [1]. HOCs are extensively synthesized and applied in agriculture and various industries [2]. Besides, numerous kinds of HOCs have been observed that are present as industrial synthetic intermediates and disinfection byproducts [3]. The high electronegativity of halogen groups (Cl, Br, F, etc.) results in a low electron cloud density around hydrocarbon chains or aromatic rings of the HOC chemical structure, and therefore, HOC is more inclined to be reductively transformed than oxidative decomposition in the environment [4]. On the other hand, the emission of HMs has been widely observed due to their extensive use in various industries, such as metal smelting, electroplating, electrical appliance manufacturing, and leather processing [5]. Certain heavy metal ions with higher valence, such as selenium (Se), uranium (U), chromium (Cr), etc., exhibit elevated electronic affinity, making them highly amenable to be reductively converted. The chemical reduction of HM ions from higher to lower valence facilitates their conversion from water-soluble forms to precipitates by combining with anions, ultimately leading to their effective removal from aqueous solutions [6].

Zero-valent iron (ZVI) is a reactive transition metal with a reductive property of −0.44 V (vs. standard redox potential) [7]. Due to its environmentally friendly and cost-effective nature [8], ZVI shows a promising functional material for the reductive removal of various persistent pollutants in the environment, including HOCs [9], nitroaromatic hydrocarbons [10], dyes [11], phenolic compounds [12], HMs [13], etc. However, the widespread application of ZVI has been hindered by several limitations [14]. In

* Corresponding author.
E-mail address: lzlhit@163.com (Z. Li).

https://doi.org/10.1016/j.ese.2024.100417

aquatic environments, the hydrogen evolution of ZVI results in significant electron consumption and the formation of a passive layer on the surface consisting of iron oxides and hydroxides, as depicted in equation (1) [15]. This layer restricts the flow of electrons from the iron reservoir to the oxide shell, thereby reducing the reactivity of iron and the life of the reaction due to an increase in the pH of the reaction medium [16]. Although previous studies have employed various strategies to enhance ZVI performance, such as using ZVI nanoparticles [17], catalytic bimetals (e.g., Pd-Fe, Ni-Fe, Cu-Fe) [18], or employing weak magnetic fields (WHF) [19], these methods face several challenges such as the nanoparticle aggregation, the potential bio-toxicity, the high cost of noble metals, and the additional energy consumption [20].

$$Fe^0 + 2H_2O \rightarrow Fe^{2+} + H_2 + 2OH^- \quad (1)$$

With the rapid progress in materials science, nonmetallic modifying methods have recently emerged to enhance ZVI's structure and functionality [21]. These studies focus on the incorporation of heteroatoms (C, N, S, P, etc.) with varying hydrophobicity and conductivity, aiming to achieve the following objectives: (i) decreasing the formation of passive metal layers brought by iron hydrolysis, thereby enhancing electron selectivity; (ii) improving the electronic structure of the particle surface to induce charge redistribution and improve electron transfer efficiency (EE) [4]. EE can be defined as the percentage of electrons used for substrate reduction (N_e) compared to the total electrons consumed (N_t) within a given time interval, as shown in equation (2) [22,23]. On account of the effective optimization of ZVI performance under the premise of low cost and green strategy, the nonmetallic modified ZVI (NM-ZVI) based principles and techniques have represented broad prospects concerning the iron reduction field for pollution control and remediation [24].

$$EE = \frac{N_e}{N_t} \quad (2)$$

According to a literature analysis using the Web of Science, studies related to NM-ZVI have experienced a peak in the past five years. Despite the ongoing changes, there has been a threefold increase in articles addressing the reductive removal of HMs in contrast to those focusing on HOCs since 2020 (Fig. 1a). Among the nonmetallic atom types, carbon modifications possessed the highest representation (52.76%), followed by boron and sulfur (Fig. 1b). Although several review articles on NM-ZVI have been published in recent years, most focus on individual types of NM-ZVI [5], such as sulfur-modified ZVI or biochar-modified ZVI [14,15]. Furthermore, these articles primarily concentrate on pollutant removal and reaction mechanisms [13,20], and a comprehensive overview of the recent advancements in technologies based on non-metallic modified ZVI remains an open field. Therefore, this review provides comprehensive insights and prospects regarding the research status, mechanisms, and potential applications of NM-ZVI for the remediation of HOCs and HMs in aquatic systems. The main contents include: (i) summarizing the developed methods for NM-ZVI preparation and evaluating their respective effectiveness; (ii) reviewing studies related to the regulation strategies by a nonmetallic modification to enhance the reductive removal efficiency of HOCs and HMs, focusing on improving the reactivity, electron selectivity and EE; (iii) elucidating the reduction dominated mechanisms involved in NM-ZVI removal of HOCs and HMs; and (iv) identifying current challenges and providing perspectives on the application of NM-ZVI during remediation of persistent pollutants.

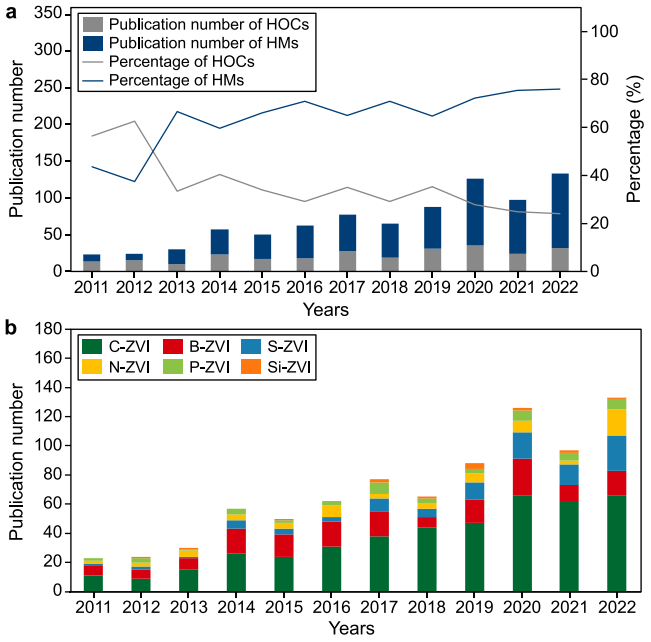

Fig. 1. **a**, Publications related to NM-ZVI between 2011 and 2022. **b**, Publications related to ZVI with modifying the different types of nonmetallic elements during the reductive removal of HOCs and HMs between 2011 and 2022.

2. Developed methods for NM-ZVI preparation and their respective effectiveness

Current methods for preparing NM-ZVI primarily involve introducing nonmetallic elements onto the surface or within ZVI [24]. Various physical and chemical preparation methods, including liquid-phase reduction, mechanical ball milling, and pyrolysis, have been employed, as shown in (Fig. 2). These different methods have distinct effects on the modifying efficiency and properties of ZVI. For instance, liquid-phase reduction allows control over the size and dispersion of metal nanoparticles, while mechanical ball milling enables heterogeneous and localized modification [25]. In addition, pyrolysis can facilitate the large-area uniform modification. When selecting a preparation method, factors such as the modifying effect, production cost, and operational complexity should be comprehensively considered [26].

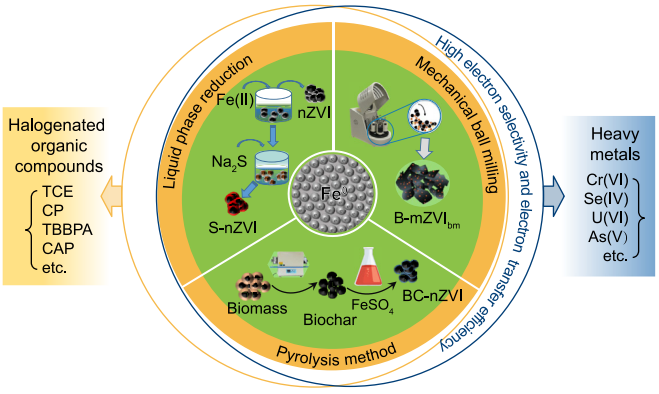

Fig. 2. Current applied preparation methods of NM-ZVI for efficiently reducing HOCs and HMs.

2.1. Liquid phase reduction method

Liquid phase reduction involves the addition of metal salts and reducing agents to an aqueous solution, resulting in the reduction of metal ions into metal nanoparticles. This method can generate suspended nZVI by reducing Fe^{2+} or Fe^{3+} in water with BH_4^- or directly depositing the nanoparticles onto the surface of loading carriers [27]. Liquid-phase reduction is advantageous for its ability to control the size and dispersion of metal nanoparticles. However, it is considered limited for large-scale production. Additionally, BH_4^- poses risks of reacting with water, leading to lower yields and the incorporation of impurities, thereby reducing the efficiency of ZVI reactions [28]. Despite these limitations, numerous studies have demonstrated the high efficiency of liquid-phase reduction for the removal of trichloroethylene (TCE), chlorophenols, chloramphenicol, Cr(VI), U(VI), etc. (Tables 1 and 2). For instance, Han and Yan [32] prepared sulfur-modified nZVI (S-nZVI) by this method, exhibiting improved reactivity and stability across a wide pH range compared to nZVI. The complete removal of TCE in water was observed within a short period. Similarly, Xu et al. [72] observed a remarkable improvement in TCE dechlorination efficiency using S-nZVI, with TCE removal efficiency increased by 160 times higher than that of pure nZVI. Li et al. [34] prepared biochar-supported modified nanoscale ZVI with a TCE dechlorination efficiency achieved 79.0% within 15 h, compared to only 11.0% of dechlorination by unmodified nZVI under the same condition. These results highlighted the remarkable effectiveness of the preparation method employed.

2.2. Mechanical ball milling method

Mechanical ball milling is a process that utilizes the continuous friction and collision between grinding balls and raw materials in a ball mill to produce particles with smaller average sizes. This method requires less solvent and generates fewer wastes, making it a simpler and cleaner approach [73,74]. Besides, this method can create novel materials that were previously difficult or impossible to synthesize, enabling the potential large-scale production [75,76].

Mechanochemical ball milling has emerged as a suitable method for nonmetallic modifying, involving the simultaneous milling of ZVI and nonmetallic elements in a ball mill. Several studies have confirmed the effectiveness of NM-ZVI prepared by applying this method for the reduction of HOCs (e.g., TCE, chlorophenols) or Cr (VI) (Tables 1 and 2). Li et al. [63] found that S-ZVI prepared through mechanical ball milling exhibited significantly improved Cr (VI) reductive efficiency, with an EE of 14.6%, approximately 10.7 times higher than unmodified ZVI. This increased EE and reactivity could be attributed to the direct solid-phase reaction between ZVI and elemental sulfur powder, leading to the formation of sulfur-iron compounds on the ZVI surface and a

Table 1
Comparison of the different preparation methods of NM-ZVI for reductive dehalogenation of HOCs.

Preparation methods	Treatment	Target pollutants	Dosage ($g\ L^{-1}$)	Initial concentration ($mg\ L^{-1}$)	Duration	Initial pH	Temperature (°C)	Removal efficiency (%)	Removal rates per g NM-ZVI (h^{-1})[a]	Reference
Liquid phase reduction	S-nZVI	Trichloroethylene	1.0	9170.0	8.0 d	5.0	25 ± 2	100.0%	47.76	[29]
	S-nZVI	Trichloroethylene	0.3	262.0	7.0 d	6.0	22 ± 2	99.0%	6.18	[25]
	S-nZVI	Trichloroethylene	1.0	9170.0	10.0 d	6.0	22 ± 2	72.1%	27.55	[30]
	S-nZVI	Trichloroethylene	2.0	14.4	6.5 h	9.0	22 ± 2	58.0%	0.64	[31]
	S-nZVI	Trichloroethylene	5.0	25.0	7.2 h	7.8–8.2	22 ± 1	90.0%	0.63	[32]
	S-nZVI	Trichloroethylene	0.3	298.7	8.0 d	8.0	25 ± 1	70.0%	4.36	[33]
	nZVI/BC	Trichloroethylene	0.1	30.0	200.0 min	7.0	20 ± 1	90.0%	81.00	[34]
	S-nZVI/BC	Trichloroethylene	3.0	20.0	2.0 h	5.8	25	100.0%	3.33	[35]
	S-nZVI	Florfenicol	1.0	36.7	2.0 h	7.0	25	16.0%	2.93	[36]
	S-nZVI	Tetrabromobisphenol A	2.3	20.0	24.0 h	N/A[b]	25	90.0%	0.33	[37]
	ZVI/AC[c]	Pentachlorophenol	0.2 ± 0.1	5.4	6.5 d	5.0 ± 0.2	25 ± 2	53.0%	0.09	[38]
	SiO_2-ZVI	2,4-Dichlorophenol	3.0	150.0	28.0 h	2.7	25	45.0%	0.80	[39]
	S-nZVI/MC[d]	Trichlorophenol	2.0	30.0	2.0 h	4.0	N/A	90.0%	6.75	[27]
	S-nZVI	Diclofenac	3.0	10.0	70.0 min	6.5	25	73.5%	2.10	[40]
	nZVI/BC	Chloramphenicol	1.1	1001.3	12.0 h	4.0–4.5	25	100.0%	78.72	[41]
Mechanical ball milling	ZVI/AC	Trichloroethylene	0.2	1.0	24.0 h	7.0	N/A	100.0%	0.21	[42]
	S-mZVI	Trichloroethylene	0.2	248.9	12.0 h	7.0	N/A	80.0%	3.33	[26]
	S–N-mZVI	Trichloroethylene	10.0	13.1	4.0 h	7.0	25	47.6%	0.16	[24]
	mZVI/AC	Trichloroethylene	10.0	50.0	8.0 h	7.0	23	90.0%	0.56	[43]
	N-nZVI	Trichloroethylene	3.0	10.4	30.0 min	N/A	25 ± 2	100.0%	6.93	[44]
	P-mZVI	Trichloroethylene	5.0	10.0	240.0 h	N/A	N/A	100.0%	0.01	[45]
	SiO_2-ZVI	2-Chlorophenol	40.0	50.0	2.0 h	3.0	25 ± 2	99.1%	0.62	[46]
Pyrolysis	N-nZVI	Trichloroethylene	1.0	20.0	5.0 d	N/A	22 ± 1	100.0%	0.17	[47]
	ZVI/BC	Trichloroethylene	2.0	9.2	65.0 min	4.5	22 ± 1	100.0%	4.23	[48]
	nZVI/BC	Trichloroethylene	5.0	30.0	4.0 h	6.3	25	97.3%	1.46	[49]
	ZVI/AC	Trichloroethylene	20.0	100.0	1.0 h	N/A	25	90.0%	4.50	[50]
	nZVI/BN[e]	Decabromodiphenyl oxide	2.5	1.0	24.0 h	N/A	25	100.0%	0.02	[51]
	nZVI/G[f]	Trichloronitromethane	0.1	0.1	2.0 h	N/A	25	99.0%	0.83	[52]
	ZVI/BC	Dichlorophenol	100.0	55.2	24.0 h	4.0	N/A	47.0%	0.01	[53]

[a] Removal ratios of 1 g NM-ZVI (h^{-1}) was calculated by the initial concentration of pollutant multiply by removal efficiency and dividing by dosage and duration.
[b] N/A indicates unavailable.
[c-f] AC, MC, BN and G indicated activated carbon, mesoporous carbon, boron nitride, and graphene, respectively.

Table 2
Comparison of the different preparation methods of NM-ZVI during reduction of high-valent HMs.

Preparation methods	NM-ZVI types	Target pollutants	Dosage ($g\ L^{-1}$)	Initial concentration ($mg\ L^{-1}$)	Duration	Initial pH	Temperature (°C)	Removal efficiency (%)	Removal rates per g of NM-ZVI (h^{-1})[a]	Reference
Liquid phase reduction	nZVI/CNT[b]	Cr (VI)	0.2	20.0	2.0 h	7.0	N/A[c]	98.0%	49.00	[54]
	nZVI/SC[d]	Cr (VI)	0.1	20.0	5.0 h	2.0	50	100.0%	57.14	[55]
	nZVI/G	Cr (VI)	1.0	25.0	3.0 h	3.0	25	80.0%	6.67	[56]
	ZVI/SF[e]	Cr (VI)	2.5	40.0	2.0 h	5.2	20 ± 1	88.0%	7.04	[57]
	nZVI/SRC[f]	Cr (VI)	0.2	30.0	24.0 h	3.0	25 ± 1	89.0%	5.56	[58]
	A[g]-BC-nZVI	U (VI)	0.1	23.6	400.0 min	6.0	25	90.0%	31.86	[59]
	S-nZVI/BC	U (VI)	0.1	10.0	12.0 h	5.0	25	80.6%	13.43	[60]
	NBC[h]-nZVI	Se (IV)	1.0	50.0	12.0 h	3.0	25 ± 1	60.5%	2.52	[61]
	nZVI/BC	Cr (VI)	4.0	50.0	24.0 h	6.0 ± 0.2	30	66.7%	0.35	[62]
Mechanical ball milling	S-ZVI	Cr (VI)	0.5	2.0	45.0 min	6.0	25	47.3%	2.52	[63]
	mZVI/BC	Cr (VI)	2.0	30.0	72.0 h	5.5	20 ± 1	97.8%	0.20	[64]
	mZVI/AC	Cr (VI)	1.0	10.0	2.0 h	3.0	N/A	94.0%	4.71	[65]
	B-mZVI	Cr (VI)	2.0	5.0	20.0 min	3.0–9.0	N/A	100.0%	7.50	[66]
Pyrolysis	P-nZVI/BC	Cr (VI)	0.8	20.0	15.0 d	2.0	30	99.4%	0.07	[67]
	ZVI/OMC[i]	Cr (VI)	1.0	50.0	10.0 min	5.6	25	99.0%	297.00	[68]
	ZVI/C[j]	Cr (VI)	1.0	10.0	3.0 d	N/A	N/A	90.0%	0.13	[69]
	nZVI/BC	Cr (VI)	1.5	10.0	4.0 h	4.0	25	96.0%	1.60	[70]
	nZVI/SB[k]	As (V)	10.0	20.0	24.0 h	2.0	25	99.0%	0.08	[71]

[a] Removal ratios of 1 g NM-ZVI (h^{-1}) was calculated by the initial concentration of pollutant multiply by removal efficiency and dividing by dosage and duration.
[b,d-k] CNT, SC, SF, SRC, A, NBC, OMC, C, nZVI/SB indicated carbon nanotube, microspherical carbon, silica fume, silicon rich biochar, active, N-doped biochar, ordered mesoporous carbon, carbon, and biochar prepared by co-pyrolysis of nano-zero-valent iron and sewage sludge, respectively.
[c] N/A indicates unavailable.

uniform distribution of Fe and S within the particles. Consequently, mechanical ball milling could effectively prevent the accumulation of iron materials [26,77]. Furthermore, nitrogen modification was proven to increase the surface area and electronic conductivity of ZVI, while sulfur modification changed the surface properties of ZVI and promoted the formation of sulfide species. Gong et al. [24] observed a synergistic effect of nitrogen and sulfur co-modification through mechanochemical ball milling, which increased the electron transfer capacity and the surface area. They enhanced the adsorption and dechlorination capacity of TCE.

2.3. Pyrolysis method

Pyrolysis is a thermal decomposition method to synthesize NM-ZVI from a mixture comprising metal salts and nonmetallic elements. This method enables NM-ZVI generation with higher quality and a narrower size distribution. During the process, an iron precursor, which can be either an iron oxide or an iron salt, is subjected to reduction by a gas-reducing agent at temperatures exceeding 500 °C. The resulting particle size and distribution depend on several crucial factors, including the precursor/top ratio, the heating rate, the final reaction temperature, and the annealing time. Common reducing agents for NM-ZVI synthesis include N_2, H_2, CO, and Ar gas [78]. When carbon-based materials like biochar or carbon black are employed for thermal decomposition, the overall synthesis process is called carbothermal decomposition or reduction. Previous studies have successfully utilized pyrolysis to synthesize various types of modified ZVI composites for reductive dechlorination of TCE and chlorophenol, reduced Cr(VI) and Arsenic (As), etc. Examples include carbon-supported modified ZVI [69], phosphorylated ZVI/BC [67], and biochar prepared through co-pyrolysis of nZVI and sewage sludge [71]. Pyrolysis-assisted synthesis offers a uniform modifying approach to NM-ZVI.

Removal or reduction efficiencies by the different employed methods were further discussed by calculating the removal ratio by homogeneous calculation (Tables 1 and 2). TCE and Cr(VI), two typical kinds of the most extensively studied pollutants, were selected for comparative analysis among the above three preparation methods. Regarding TCE removal, liquid-phase reduction showed the highest removal ratio, with TCE reductive dechlorination rates approaching 81.0 h^{-1} per g NM by biochar modification and 47.8 h^{-1} per g NM by sulfur modification, respectively. Additionally, nitrogen-modified ZVI represented the TCE reductive dechlorination rate of 6.9 h^{-1} per g NM, followed by sulfur and carbon co-modified materials (6.6 h^{-1} per g NM) via liquid-phase reduction. For Cr(VI) removal, the highest reduction rate of 297.0 h^{-1} was confirmed using pyrolysis preparation, which was the highest among all studies. Besides, ZVI modified with two carbon materials, carbon nanotube and micro spherical carbon, prepared by liquid-phase reduction methods, also showed comparatively higher reductive dechlorination efficiencies of 49.0 and 57.1 h^{-1} per g NM, respectively. According to the summarized data of current studies, the liquid-phase reduction generally exhibited superior removal performance for both HOCs and HMs. However, it might be limited, considering the scale of the application. The ball milling method possessed green characteristics and large-scale application potential, and the overall removal efficiency was relatively low. Pyrolysis occasionally showed extremely high removal efficiency, which might depend on the specific preparation details.

Based on Tables 1 and 2, the impacts of different NM-ZVI on the reductive removal of HOCs and HMs are further discussed. Among the six distinct non-metallic element modifications, two extensively studied pollutants, TCE and Cr(VI), were chosen for comparative analysis. Regarding TCE removal, biochar modification exhibited the highest removal rate, followed by sulfur and nitrogen modifications. In removing Cr(VI), ordered mesoporous carbon modification showed the highest reduction rate, followed by sulfur and biochar co-modification and boron modification. According to the current research data, carbon-modified ZVI exhibited superior removal efficiency for HOCs and HMs, followed by sulfur modification.

3. Regulation strategies of ZVI reactivity by nonmetallic modifying

Recent advancements in the NM-ZVI principle aim to disrupt the passivation film on the original ZVI surface layer and enhance the reactivity during prolonged applications. The reduction-dominant mechanisms involved in removing HOCs and HMs by NM-ZVI encompass various pivotal processes. These include intricate interactions among electron transfer reactions, surface modifications, and catalytic processes. The reduction process typically occurs through electron transfers from NM-ZVI to pollutants. ZVI acts as an electron donor to reduce HOCs and HMs, converting them into less harmful or inert forms. Furthermore, surface reactions between modified ZVI and pollutants play a crucial role; the modified surface of ZVI enhances pollutant adsorption, bringing pollutants closer, thereby enhancing selectivity and reactivity and consequently promoting their reduction. Specific active sites or intermediate products formed on the modified ZVI surface contribute to catalyzing pollutant degradation.

The selection of element types and ways of modifying play critical roles in regulating the different physicochemical properties of ZVI, such as surface electronic structure, hydrophobicity, specific surface area, crystal structure, etc. [36,72]. The material property would directly determine the system's reactivity and longevity. For example, nonmetallic elements (C, N, S, P, etc.) could form chemical bonds with Fe on the ZVI surface, and their distinct electronegativities would adjust the surface charge distribution and electron affinity of ZVI [30]. A nonmetallic modification was also able to modify the crystal structure of ZVI and reduce the electron transfer resistance [66]. In sum, based on the currently reported principles, the following three strategies were frequently applied in the NM-ZVI reaction system to improve the reactivity: (i) controlling the modifying element types, (ii) adjusting the element content ratio, and (iii) increasing the lattice constant, with the schematic diagram as described in (Fig. 3).

3.1. Modifying with the different types of nonmetallic elements

3.1.1. Carbon-modified ZVI

Carbonous materials, including biochar (BC) [53], carbon nanotubes (CNTs) [79], and activated carbon (AC) [38], have been utilized as modifiers of ZVI for the removal of various kinds of persistent pollutants, including polychlorinated biphenyls (PCBs), pentachlorophenol, Cr(VI), etc. [80]. The high performance achieved through modifying the carbon composites could be attributed to the more surface active sites [81], the less particle size [82], and the more dispersion [50] facilitated by the improved hydrophobicity and conductivity of carbon-modified ZVI materials. The enhanced dispersion not only boosted the reactivity of ZVI towards pollutants but also effectively mitigated the agglomeration of nZVI particles [83].

Multiple studies demonstrated the efficacy of carbon-modified ZVI composites in removing pollutants. Adding carbon contributed to increased active surface sites, improved adsorption, and facilitated reductive dechlorination and precipitation reactions to remove contaminants. For instance, Cao et al. [79] investigated using nZVI/CNT composites for PCB removal and observed an appropriate 30% increased removal efficiency compared to the pure nZVI upon biochar addition. The increased active surface sites provided by CNT greatly improved the adsorption and reductive dechlorination activity. Ren et al. [38] found that ZVI/AC composites exhibited twice the removal efficiency of pure nZVI for pentachlorophenol removal. Additionally, carbonate and phosphate groups in biochar could form insoluble precipitates with metal cations, effectively immobilizing them and providing additional active surface sites for the removal of HMs, such as U(VI) and Cr(VI) [62,84]. Pang et al. [60] observed the biochar-modified ZVI could efficiently remove U(VI) from aqueous solutions by forming the insoluble precipitates with metal cations. The introduction of biochar not only improved the dispersion of S-nZVI but also assumed the adsorption role in U(VI) capture, with S-nZVI/BC adsorbing 2.4 times more U(VI) than S-nZVI and 3.8 times more than nZVI. Wang et al. [65] discovered the addition of biochar to nZVI composites greatly enhanced the removal efficiency of Cr(VI) in aqueous solution, achieving a 97.8% of removal efficiency. In the presence of Fe^0, graphitized structure in 700 °C ball milled biochar acted as an electron conductor, facilitating electron transfer from Fe^0 to Cr(VI). Ball milling also destroyed the surface iron oxide layer to regenerate the composite (Fig. 4a).

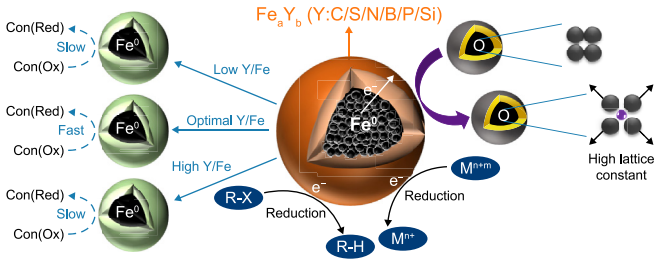

Fig. 3. Schematic diagram of regulation strategies of NM-ZVI to optimize the reactivity.

3.1.2. Sulfur-modified ZVI

The main principles of sulfidation involved modifying the surface morphology of ZVI to increase the hydrophobicity and prevent aggregation, and forming a FeS_x structure on the ZVI surface layer [31,85]. The presence of FeS_x served two purposes: (i) directly participating in the reductive removal of persistent pollutants and (ii) leading to a substantial redistribution of surface charge density to create a highly active surface that facilitated reactions with targeted pollutants [36]. Based on the superior reactivity and activity, the sulfured ZVI has exhibited excellent reductive efficiencies for various kinds of volatile chlorinated hydrocarbons (VCHs), as well as HMs, including Cr(VI), As(V), or U(VI) [29,36,71]. Zhang et al. [86] demonstrated that nZVI after sulfidation caused an improved maximum degradation efficiency of 3.1–24.4-fold for all kinds of VCHs under electron-limited conditions. Sulfidation prevented the generation of intermediate dechlorination products and favored a degradation pathway that led to non-chlorinated benign products, which was beneficial for the remediation of groundwater contaminated with mixtures of VCHs (Fig. 4b). Kim et al. [87] found the sulfidated FeS_x/nZVI particles exhibited an up to five times higher reactivity towards TCE compared to the untreated nZVI. Fan et al. [88] observed the sulfidated ZVI demonstrated up to 2.6 times higher reactivity towards TCE in the presence of sulfur-containing materials. Fan et al. [89] reported the sulfidated ZVI achieved a much higher removal efficiency (41%) of Se (VI) compared to the sulfur-modified ZVI (4%) under identical conditions.

3.1.3. Nitrogen-modified ZVI

Nitrogen-modified ZVI (N-ZVI) could obtain superior particle reactivity and improved corrosion resistance compared with carbon and sulfur modification. Some studies have verified that nitrogen-containing functional groups were crucial in capturing metal cations in water, facilitating mass transfer, and promoting electron attachment from the iron core to the surface, accelerating reductive efficiencies [61,90]. Several studies found that incorporating nitrogen into nZVI formed the iron nitride (Fe_xN) phase, which created additional active sites and enhanced the reactivity

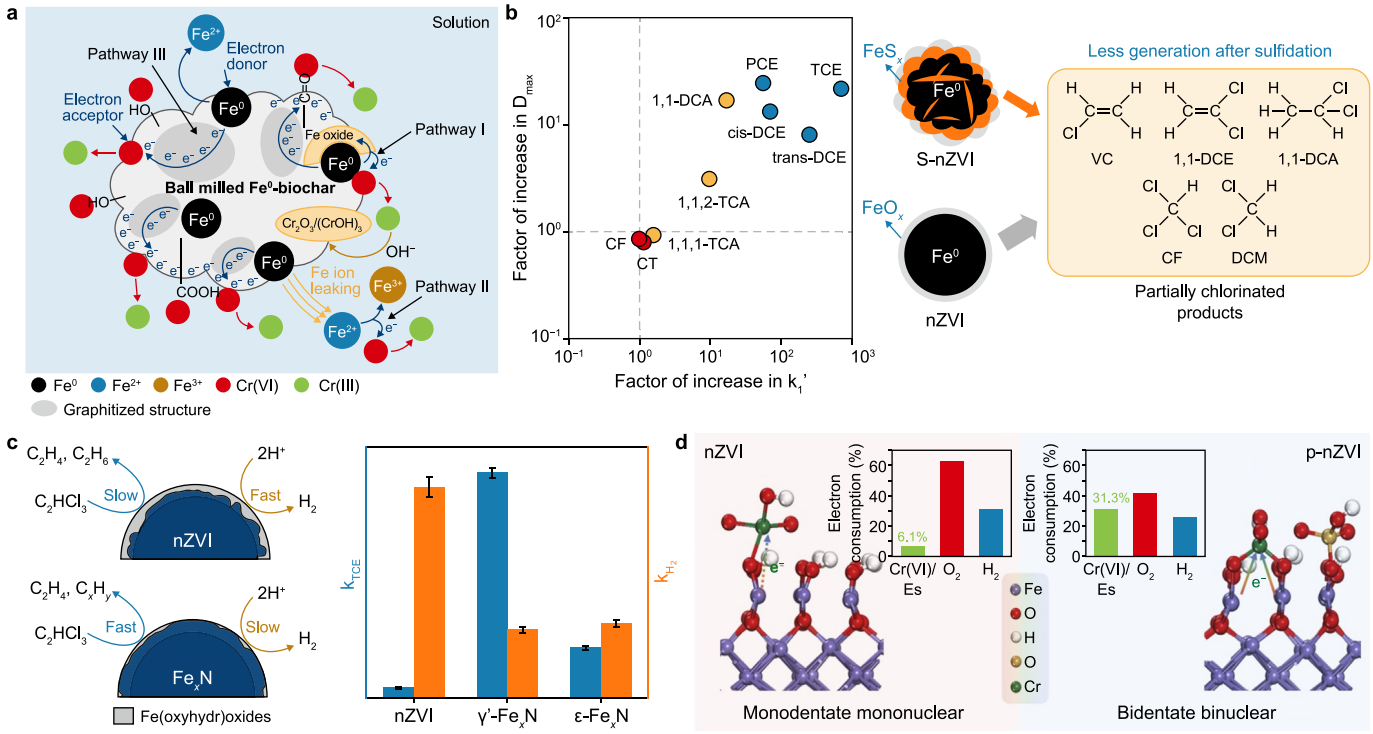

Fig. 4. **a**, Aqueous Cr(VI) removal by a novel ball milled Fe^0-biochar composite: the role of biochar electron transfer capacity under high pyrolysis temperature. Adapted with permission from Ref. [65]. Copyright 2019, Elsevier B.V. **b**, A comprehensive assessment of the degradation of C1 and C2 chlorinated hydrocarbons by sulfidated nanoscale zerovalent iron, Adapted with permission from Ref. [86]. Copyright 2021, Elsevier B.V. **c**, Iron nitride nanoparticles for enhanced reductive dechlorination of trichloroethylene [47]. **d**, Phosphate modification enables high efficiency and electron selectivity of nZVI toward Cr(VI) removal, Adapted with permission from Ref. [94]. Copyright 2019, Elsevier B·V.

towards HOCs [44]. Moreover, the modification of microstructure and the formation of a covalent bond between the lone-pair electrons of nitrogen and the empty orbit of iron significantly contributed to the decreased iron corrosion, which was vital for the effective and environmentally sustainable long-term remediation [89]. Brumovský et al. [47] observed the face-centered cubic (γ′-Fe_4N) and hexagonal close-packed (ε-$Fe_{2-3}N$) arrangements of modified ZVI nanoparticles exhibited a 20- and 5-fold increased TCE dechlorination rate, compared to the pristine nZVI, as well as an approximately 3-fold decreased hydrogen evolution rate. TCE dechlorination experiments with aged particles showed that the γ′-Fe_4N nanoparticles retained a high reactivity after three months of aging. A low energy barrier of 27.0 kJ mol^{-1} for the first dechlorination step of TCE on the γ′-Fe_4N surface was revealed, representing a novel and potentially important approach for reductive dechlorination of TCE (Fig. 4c).

3.1.4. *Modified ZVI with the other types of elements*

The outstanding performance of boron-modified ZVI (B-ZVI) could be attributed to introducing the lattice strain and modulation of the electron structure, thereby creating active sites with increased electron affinity and reactivity [66,92,93]. Moreover, B-ZVI exhibited remarkable corrosion resistance. Wei et al. [66] found the interstitial boron induced tensile strain in the iron core, destabilized the FeO_x layer, and facilitated the more iron core electrons crossing the Ohmic interface of Fe-FeO_x, thus leading to a wider electron accumulation zone in the FeO_x layer. Boron-modified ZVI caused the increase in both the electron supply rate by 13 times and the kinetic constant of Cr (VI) removal by 63 times.

Phosphorus-modified ZVI (P-nZVI) significantly enhanced the reductive efficiencies through various mechanisms, including enhancing active surface sites, suppressing undesired reactions, altering adsorption configurations, and providing additional electron transfer pathways [45,94,95]. Li et al. [45] found phosphorization limited the circumferential stress of nZVI particles and caused the numerous radial nanocracks by “breaking” the compact spherical structure, which facilitated the inward diffusion of HMs, the outward transfer of electrons and Fe^{2+}, and the interfacial electron exchange. Li et al. [94] demonstrated a fourfold increase in the removal efficiency of Cr (VI) by applying P-nZVI, with an electron efficiency increasing from 6.1% to 31.3%, five times higher than that of nZVI. Phosphate groups adsorbed on the P-nZVI surface in a monodentate manner, effectively suppressing the undesirable reactions of ZVI with oxygen or water. Additionally, the adsorption configuration of Cr (VI) on P-nZVI was shifted from monodentate to bidentate, therefore favoring the electron transfer through dual channels and causing the higher electron transfer efficiency for Cr (VI) adsorption and reduction (Fig. 4d).

Silicon dioxide-modified ZVI (SiO_2-nZVI) offered multiple advantages in improving the dispersibility, reactivity, and reduction of ZVI. Firstly, the silica coating enhanced the stability of ZVI by improving the resistance to oxidation and corrosion, thereby prolonging the operational lifespan [96]. Secondly, the silica layer provided additional adsorption sites, augmenting the contact area between pollutants and particles, thereby facilitating adsorption [97]. Additionally, silica modification enabled the regulation of particle size and dispersion of ZVI, optimizing the reaction conditions and enhancing the removal efficiency [98]. Zhang et al. [46] synthesized silica-modified ZVI composites, achieving a highly active 2-chlorophenol dechlorination efficiency. Salama et al. [99] reported that SiO_2-nZVI exhibited a remarkably high reductive efficiency of 96.8% for Cr (VI) from water.

The differences among these various NM-ZVI types reside in their elemental alterations, conferring distinct pollutant

remediation properties. Carbon-modified ZVI enhances adsorption and reductive potential, while sulfur modification increases hydrophobicity and prevents aggregation. Nitrogen modification augments corrosion resistance and metal cation adsorption, heightening reactivity. Boron modification alters electron structure and increases active sites, phosphorus modification alters adsorption configurations, strengthening active sites, and silicon dioxide modification improves dispersibility, stability, and adsorption points, enhancing removal efficiency. The selection of NM-ZVI types hinges on several parameters: pollutant specificity determines the choice (e.g., HOCs or HMs), requisite reactivity defines the suitable modification, and the demanded operational lifespan and ecological sustainability influence the selection for efficient and environmentally responsible remediation in specific environments. Choosing the type of NM-ZVI considers their distinct characteristics to achieve optimal pollutant removal while addressing practical applicability and environmental concerns.

3.2. Controlling the content ratio of nonmetallic elements

The insufficient nonmetallic content would cause incomplete coverage of the iron surface, and the excessive content might block the active sites, reducing the reactivity and the reductive efficiency [100]. Therefore, determining the optimal ratio of nonmetallic elements to iron was crucial for ensuring the efficient reduction of HOCs and HMs [88]. However, the specific optimal ratio depended on multiple factors, including the reaction system, the nonmetallic element types, and the nature of the target contaminants [17]. Thus, a balance between nonmetallic and iron elements is necessary to maintain highly efficient reductive activity.

Kim et al. [101] found the insufficient sulfur content resulted in incomplete FeS coverage, while the excessive sulfur content led to the formation of FeS_2, which exhibited a lower reactivity towards the target pollutants, such as Cr(VI) and TCE, compared to FeS. Rajajayavel and Ghoshal [31] observed the sulfidation nZVI to different extents (Fe/S molar ratios 0.62–66) caused the surface-area normalized first-order TCE dechlorination rate constant k increase up to 40 folds. The Fe/S molar ratios in the range of 12–25 offered the highest TCE dechlorination rates and decreased at either higher or lower Fe/S. Gong et al. [102] reported a remarkable 63.0% increase in Cr(VI) removal efficiency under an optimal S/Fe molar ratio of 0.21. Song et al. [40] indicated that a suitable S/Fe ratio of 0.3 improved Diclofenac (DCF) dechlorination efficiency by 73.5%. Su et al. [103] found that the S/Fe ratio strongly influenced the Cd (II) removal performance of S-nZVI, with a 50% improvement under a S/Fe ratio of 0.28. Gong et al. [91] identified an optimal N/Fe molar ratio of 0.05, where N–C-mZVI$_{bm}$ exhibited approximately 3.5 times higher TCE dechlorination rate than the bare mZVI$_{bm}$. Decreasing the N/Fe molar ratios results in reduced reactivity of N–C-mZVI. Conversely, excessively high N/Fe molar ratios can hinder TCE dechlorination due to the blockage and masking of reaction sites on N–C-mZVI$_{bm}$. Chen et al. [52] discovered that graphene-nZVI with a Fe/C mass ratio of 1:5 exhibited the highest trichloronitromethane (TCNM) removal efficiency, reaching 91.5% within 60 min. In comparison, TCNM removal rates decreased to 75.1%, 80.6%, and 61.3% for Fe/C with mass ratios of 1:15, 1:10, and 1:1, respectively. Meng et al. [44] observed an up to 27 times higher TCE removal rate with an N/Fe molar ratio of 0.13 for nitrogen-modified ZVI compared to an unmodified ZVI. Zhou et al. [104] reported an optimal C/Fe molar ratio of 20, which caused an 80.0% increase in EE.

Research across various studies showcased the critical role of elemental ratios in modifying ZVI for contaminant removal. Optimal ratios of sulfur-to-iron (Fe/S), nitrogen-to-iron (N/Fe), and carbon-to-iron (C/Fe) significantly impacted the reactivity and efficiency of ZVI in removing pollutants like Cr(VI), TCE, DCF, Cd(II), and TCNM. The findings revealed a delicate balance: insufficient or excessive ratios compromised the removal effectiveness, highlighting the necessity for precise control over elemental compositions in modified ZVI for optimal pollutant removal.

3.3. Increasing the lattice constant

The reductive reaction occurring with iron core electrons of ZVI involves releasing and transferring electrons. The efficiency of electron release and their subsequent transfer through nonmetallic iron (Fe_aY_b) bonds is influenced by the strength of Fe–Fe interactions and the energy level of bonding electrons at the Fe-Fe_aY_b interface. These factors are intrinsically linked to the atomic lattice of the iron core [105]. A smaller lattice constrains the release of valence electrons, necessitating higher energy, while a larger lattice constant increases the inter-atomic distance, allowing for a more efficient release of valence electrons with lower energy consumption [44,72]. Therefore, the lattice constant plays a crucial role during the electron transfer and the reactivity of the ZVI particle.

Some previous studies found the incorporation of nonmetallic elements during ZVI preparation could induce a non-uniform distribution of surface charge, improve the density of states at the Fermi level, reduce the *d*-band filling at metal sites, and shift the energy level of the *d*-band center closer to the Fermi level [15,106]. Xu et al. [29] observed Fe precursors altered the crystalline structure of both nZVI and S-nZVI. The materials made from Fe^{3+} precursor possessed an expanded lattice in the Fe^0 body-centered-cubic structure and a lower electron-transfer resistance, supporting with a higher reactivity with water (2–3 fold) and TCE (5–13 fold) than those made from Fe^{2+} precursor. The study proposed Fe and S precursors could be applied to select the conditions of the synthesis process to provide the selected physicochemical properties (e.g., S speciation, hydrophobicity, and crystalline structure), reactivity, and selectivity of the S-nZVI materials (Fig. 5a). Besides, the rational synthesis and design of robust S-nZVI by controlling the amount and morphology of sulfur in S-ZVI could lead to the lattice expansion, resulting in a larger lattice constant and a smaller atomic spacing, thus to increase the electron transfer efficiency, conductivity, and reductive capability of persistent pollutants [104] (Fig. 5b).

Gao et al. [108] demonstrated that biochar-supported sulfidated nZVI (S-nZVI/BC) significantly enhanced the reductive debromination activity of tetrabromobisphenol A, attributing to sulfur-induced expansion of Fe^0 biochar lattice constant. The S/Fe molar ratio of 0.09 in S-nZVI/BC caused the largest lattice constant, efficiently decreasing the electron transfer resistance and promoting the electron transfer efficiency. Wei et al. [66] employed an interstitial boron modification to induce tensile strain in mZVI, increasing the Fe-Fe bond length from 2.48 to 2.52 Å. Under this strained condition, 0.52 of the electron was delocalized from the iron lattice, which disrupted the stability of Fe–Fe interactions and released the trapped electrons from the iron reservoir. Boron modification altered the electronic structure and charge distribution on the iron surface, forming a stable oxide layer that effectively inhibited iron corrosion. This corrosion resistance enabled B-ZVI to maintain reactivity and longevity under complex environmental conditions. The strained mZVI demonstrated an impressive 62-fold increase in the removal rate of Cr(VI) compared to the unstrained ZVI (Fig. 5c).

The strategic integration of nonmetallic elements during ZVI synthesis emerges as a pivotal method to fine-tune the material's properties. These adjustments affect lattice expansion, electron transfer efficiency, and conductivity and play a critical role in stabilizing the surface structure. The resulting enhancements in

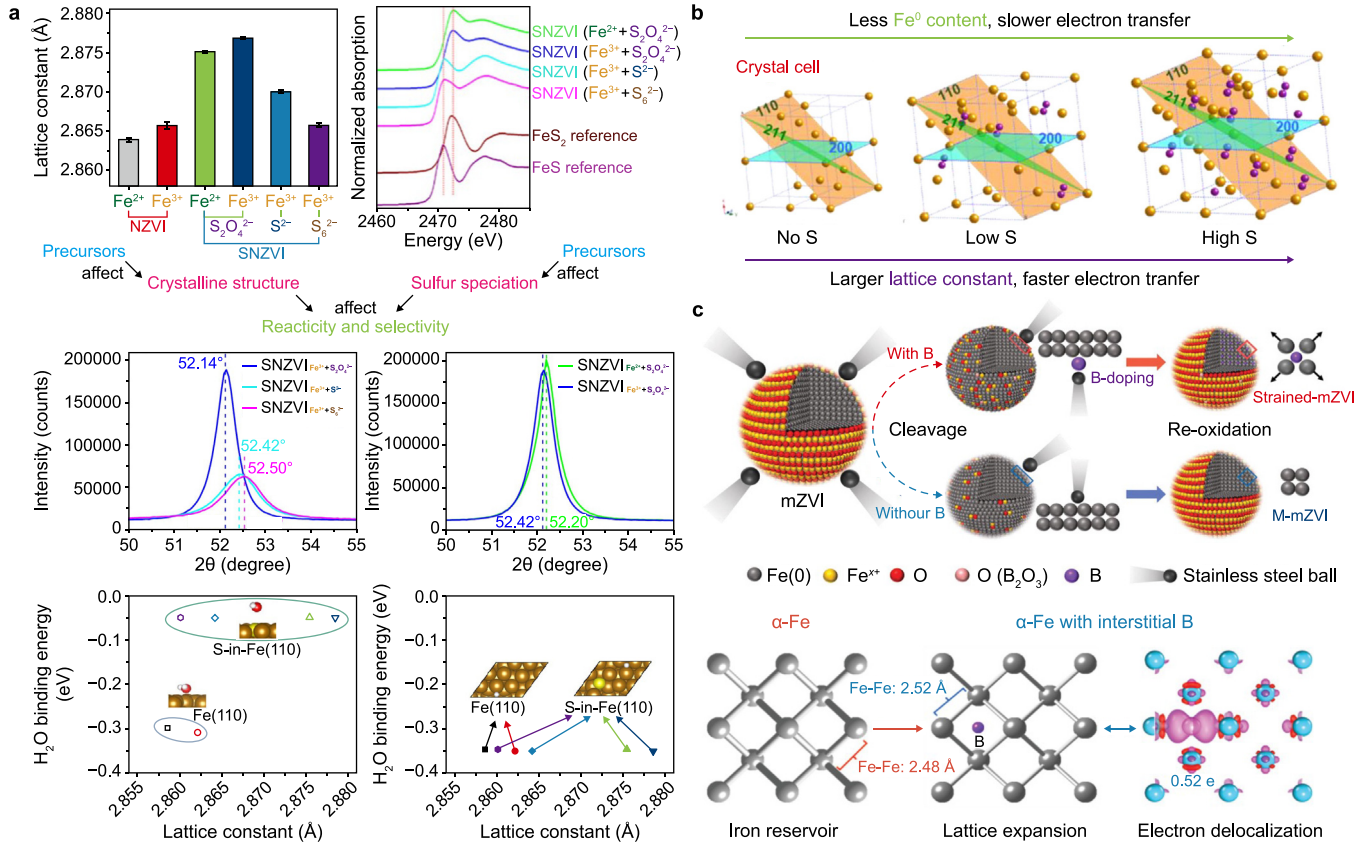

Fig. 5. **a**, Iron and sulfur precursors affect the crystalline structure, speciation, and reactivity of sulfidized nanoscale zerovalent iron, Adapted with permission from Ref. [30]. Copyright 2020, American Chemical Society. **b**, The relationship between different sulfur iron ratios and lattice constants, Adapted with permission from Ref. [107]. Copyright 2021, American Chemical Society. **c**, Influence of lattice strain on the stability and fermi level of iron nuclei, Adapted with permission from Ref. [66]. Copyright 2022, Wiley.

reactivity and durability facilitate an impressive surge in the removal rates of persistent pollutants, indicating a promising direction for tailored and highly efficient environmental remediation strategies.

4. Regulation strategies of electron selectivity and utilization efficiency of NM-ZVI

In the aqueous phase, the reaction of ZVI with water molecules is one important side reaction that holds the tendency to generate hydrogen gas and undergo corrosion. This would largely consume electrons and result in poor electron selectivity and electron utilization efficiency between ZVI and the target pollutants [109,110]. Therefore, it is crucial to develop strategies to decrease the presence of competing species like H_2O and improve electron selectivity and electron utilization efficiency [111]. Increasing the hydrophobicity is one strategy to improve electron selectivity and EE, allowing the adsorption of more target pollutants and reducing contact with water molecules, thus decreasing the likelihood of side reactions [112]. Furthermore, improving the conductivity of NM-ZVI, which could accelerate electron transfer rates and minimize side reactions, is another critical strategy for improving electron selectivity and EE [22,103,113]. Therefore, based on the principle of improving electron selectivity and EE, NM-ZVI primarily focuses on two aspects: (i) increasing the hydrophobicity and (ii) increasing the conductivity between NM-ZVI and target pollutants, as described in detail in (Fig. 6).

4.1. Improving the hydrophobicity of ZVI

The increased hydrophobicity of ZVI by nonmetallic modification could be attributed to the repulsive interaction between water and *p*-block elements, such as C, S, N, and Si, which largely reduced the water adsorption energy of ZVI [72,96]. Carbon material with high hydrophobic functional groups could effectively enhance the hydrophobic adsorption and electron transfer of persistent pollutants [114–116]. Dong et al. [49] reported that biochar pyrolysis temperature resulted in differences in surface areas, aromaticity, and noncarbonized fractions, determining hydrophobicity, electron selectivity, and reductive performance. Wang et al. [64] highlighted ball milling exposed functional groups of biochar, leading to an enhanced hydrophobicity of ZVI/BC and improved removal performance for Cr(VI). Fan et al. [117] reported that the removal rate constant of *p*-nitrophenol (*p*-NP) by ZVI modified with carbon quantum dots (C-dots @ ZVI) was 1192.7 times higher than that of ZVI alone, and the utilization of C-dots@ZVI and the EE increased by 3.7 and 2.9 times, respectively. The enhanced effect of C-dots on *p*-NP chelation by ZVI should mainly be attributed to the increased hydrophobicity of the ZVI surface, which largely facilitated the electron transfer of ZVI (Fig. 7a).

Since iron sulfides (FeS_x) exhibited a higher hydrophobicity compared to iron oxides, ZVI by sulfidation holds the potential to improve the electron selectivity by reducing the ability of non-target H_2O to compete for electrons with S-ZVI [31,118]. He et al. [33] reported the increased surface roughness and specific surface area by introducing an appropriate sulfur content, resulting in a

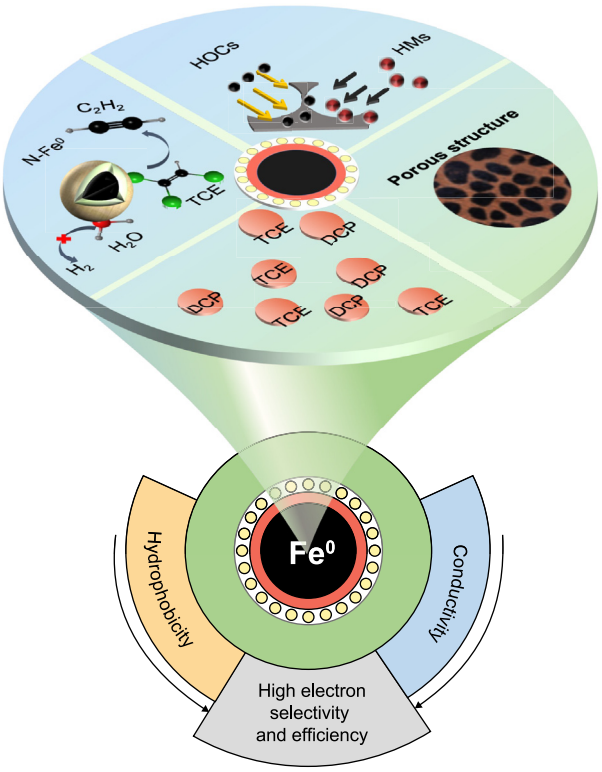

Fig. 6. Schematic diagram of regulation strategies of NM-ZVI to improve the electron selectivity and utilization efficiency.

greater hydrophobicity and a larger water contact angle for ZVI. A significant increase in the EE from 2% to 72% for TCE dechlorination was observed. Gu et al. [26] found the EE of ball-milled sulfidized ZVI (S-ZVI$_{bm}$) was nearly ten times higher than bare ball-milled ZVI (ZVI$_{bm}$). Xu et al. [72] discovered that controlling the amount and the sulfur speciation in S-nZVI could greatly improve the hydrophobicity of ZVI, which strongly improved the electron selectivity and lifetime. The nZVI sulfidation made the system highly reactive (up to 0.41 L m^{-2} d^{-1}) and selective for TCE dechlorination over water (up to 240 mol TCE per mol H_2O), with an EE of up to 70%, and these values were 54-, 98-, and 160-fold higher than for nZVI, respectively (Fig. 7b).

Following the diagonal rule of N and S in the periodic table, the nitrogenated ZVI materials were expected to exhibit improved hydrophobicity and electron selectivity compared to sulfur [118]. The addition of N to the body-centered cubic (BCC) structure of Fe^0, as reported by Meng et al. [44], enhanced the hydrophobicity of the material and accelerated the electron transfer based on theoretical calculations. The materials maintained a high electron efficiency (87.0–95.0%) due to the greatly suppressed water reactivity (109–127 times lower than un-nitridated Fe^0). Under the optimized nitridation degree, the TCE reductive dechlorination rate by nitridated Fe^0 (up to 4.8 × 10^{-2} L m^{-2} h^{-1}) was much higher (up to 27-fold) than that of un-nitridated Fe^0 (Fig. 7c).

Besides, the silica layer modified with ZVI introduced additional hydrophobic sites, thus enhancing the contact area between hydrophobic pollutants and ZVI material [97]. Wan et al. [39] investigated the selectivity of mesoporous silica-coated nZVI for the removal of 2,4-dichlorophenol (2,4-DCP) from water, demonstrating an increase in removal rate over nZVI by 45.0%. The amorphous SiO_2 coating significantly improved the corrosion resistance of nZVI and affirmed the ability to facilitate nZVI performance by mesoporous silica coating. Moreover, zeolite-supported trace zero-valent iron (Z-mZVI) exhibited a higher hydrophobic adsorption performance and reductive ability for Cr(VI) and Cd(II). The Z-mZVI realized the removal efficiency exceeding 77% for Cr(VI) and 99% for Cd(II), whereas the same amount of iron in nZVI only achieved 45% for Cr(VI) and 9% for Cd(II), respectively [98].

In addition, some studies investigated the effects of regulating the hydrophobicity and the EE of ZVI by co-modifying with two or three nonmetallic elements. Zhang et al. [119] elucidated that S-nZVI/BC exhibited a 2.6-fold higher reaction rate for removing *p*-nitrophenol (PNP) than pure nZVI. This improvement could be attributed to the dual modification of nZVI by carbon and sulfur, which reduced the energy barrier for PNP removal reactions and alleviated surface passivation. The apparent activation energy under anaerobic conditions decreased by 23.7% after sulfidation treatment, while the PNP removal efficiency increased by 8.0%. The hydrophobic nature of biochar significantly influenced the performance of S-nZVI/BC. The presence of biochar effectively mitigated particle aggregation of nZVI, thereby enhancing the dispersibility and electron selectivity of S-nZVI/BC. Gong et al. [24] described the synergistic promotion of rapid and selective electron transfer from (or surrounding) the iron oxide surface to TCE through sulfidation and nitridation. Sulfidation inhibited the hydrogen evolution reaction (HER), while pyridine nitrogen and pyrrole nitrogen, as metal coordination sites activated by their lone pair electrons, resulted in high degradation rates, electron efficiency, and dechlorination capacity. The observed rate constants (K_{obs}) and surface area-normalized rate constants (K_{SA}) of S-N(C)-mZVI$_{bm}$ were approximately five and two times higher, respectively, than those of S-mZVI$_{bm}$. Moreover, they were approximately 50 and 35 times higher than N(C)-mZVI$_{bm}$ (Fig. 7d).

4.2. Increasing the conductivity of ZVI

NM-ZVI could exhibit enhanced conductivity and electron transfer ability, probably attributed to incorporating elements that imparted the semiconducting properties of ZVI [31,42]. These semiconducting properties were able to reduce the resistance to electron transfer from the Fe^0 core to the particle surface and increase the rate of electron reduction for the target pollutants [61].

Biochar acts as an electron transfer mediator and has been utilized as a modifier for ZVI to improve the conductivity and the EE [53]. Yang et al. [83] found biochar incorporation could facilitate the electron transfer and promote the generation of Fe^{2+} ions to favor the co-precipitation of Pb^{2+}, Cu^{2+}, or Zn^{2+}. Wang et al. [64] emphasized the role of graphitic structure in ZVI/BC as an electron conductor, which enabled an efficient electron transfer from Fe^0 to Cr(VI), thereby enhancing the removal rate of Cr(VI). Carbon fibers (CF), known for their excellent electronic conductivity, significantly improved ZVI performance in reactivity and selectivity, with the TCE removal rates improving by 6.9–16.6 folds [42]. Additionally, Wu et al. [61] reported the composite material formed by loading nZVI onto the nitrogen-modified biochar (NBC-nZVI) exhibited a remarkably enhanced removal kinetic rate (143.4% of improvements) and electron utilization efficiency (15.3%) for Se(IV) removal, respectively, compared to the bare nZVI. These improvements are attributed to the positive charge, buffering effect, and excellent conductivity of NBC.

The sulfur-modified nZVI had shown superior electron transfer capacity and EE. The enhanced performance was attributed to the semiconducting or metallic conductive properties of ferrous sulfide due to the presence of ionized electrons [92]. The FeS_x and polysulfides possessed a lower bandgap than the other iron sulfides or iron oxides, enabling an efficient transition of electrons from the

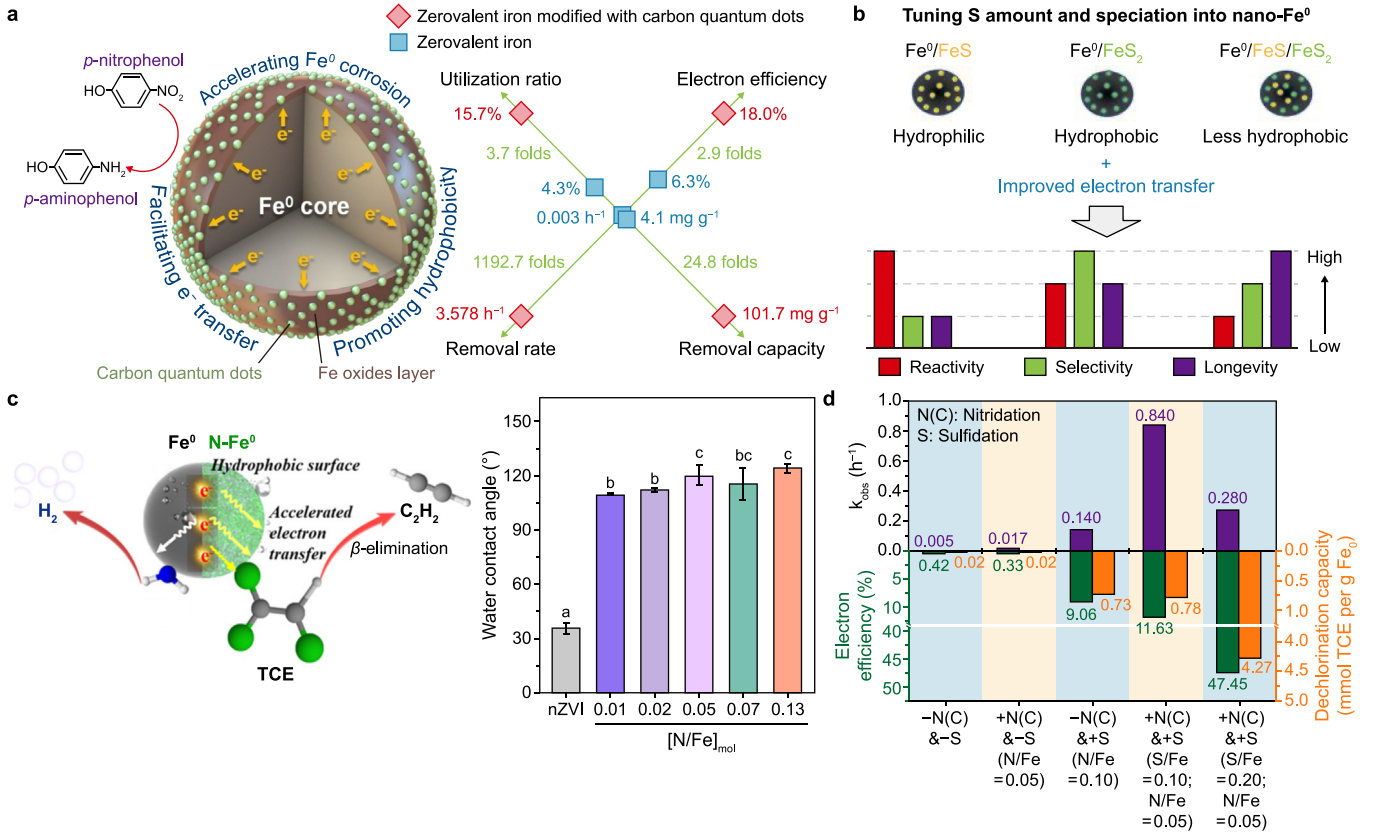

Fig. 7. **a**, Enhanced reduction of *p*-nitrophenol by zerovalent iron modified with carbon quantum dots, Adapted with permission from Ref. [117]. Copyright 2020, Elsevier B.V. **b**, Sulfur loading and speciation control the hydrophobicity, electron transfer, reactivity, and selectivity of S-nZVI, Adapted with permission from Ref. [72]. Copyright 2020, Wiley. **c**, Even incorporation of nitrogen into Fe^0 nanoparticles as crystalline Fe_4N for efficient and selective trichloroethylene degradation, Adapted with permission from Ref. [44]. Copyright 2022, American Chemical Society. **d**, Coincorporation of N and S into zero-valent iron to enhance TCE dechlorination: kinetics, electron efficiency, and dechlorination Capacity, Adapted with permission from Ref. [24]. Copyright 2021, American Chemical Society.

valence band to the conduction band. This led to higher intrinsic charge carrier concentrations and an improved conductivity than bare ZVI [93]. Consequently, the resistance to electron transfer was reduced, facilitating an electron transfer from the Fe^0 core to the particle surface [85]. Kim et al. [87] reported that S-nZVI exhibited a higher surface area and better conductivity than nZVI, enabling a removal efficiency five times higher than nZVI. Additionally, Li et al. [37] conducted the electrochemical tests and confirmed the greater electron transfer capacity and EE of S-nZVI compared to unmodified nZVI. Over 90.0% of the initial tetrabromobisphenol A was transformed by S-nZVI within 24 h, 1.6 times as high as that for the non-sulfidated nZVI.

5. Conclusions and perspective

The non-metallic modification substantially enhances ZVI performance by enhancing corrosion resistance, reducing hydrolysis and hydrogen evolution, and improving the reductive activities against high-valent HMs and HOCs. The enhanced performance is closely linked to altered physicochemical properties on particle surfaces and interiors. These changes are influenced by the modifying methods and the types and ratios of non-metallic elements used for modification. Hydrophobicity, conductivity, and lattice constants can be regulated through modification, leading to improved electron selectivity and transfer efficiency of ZVI. The simplicity and environmental friendliness of the non-metallic modification process make it an attractive strategy for improving the traditional properties and performance of ZVI, notably improving iron utilization efficiency and reductive rates. This method exhibits substantial potential for remediating persistent pollution in aquatic environments.

However, despite advancements in NM-ZVI studies, limitations and challenges demand attention. Thus, further research and development in this field are imperative to overcome these limitations and expand ZVI technology's potential applications. To address these challenges, the following research priorities are proposed.

(i) Multi-pollution collaborative reductive removal with rational-designed NM-ZVI. Current studies have focused mainly on specific pollutants, neglecting the collaborative removal of multiple pollutants. Future research should prioritize designing customized reductive systems that simultaneously target different pollutants. Regulating preparation methods and modifying elements or physicochemical properties of iron can minimize competition between active sites, facilitating selective or collaborative removal of diverse pollutants.

(ii) NM-ZVI coupled with organohalide respiration bacteria (OHRB). Integrating NM-ZVI's reductive capabilities and OHRBs' metabolic activities aims to enhance HOC removal [120]. This synergistic approach utilizes hydrogen from ZVI hydrolysis as electron donors for OHRBs. Further investigation is necessary to optimize performance and mitigate

adverse effects of NM-ZVI on bacteria using micron-sized materials or particle modification.

(iii) NM-ZVI integrated with the other oxidative processes to completely mineralize halogenated aromatics. For complex HOCs containing aromatic rings, solely relying on reductive dehalogenation for detoxification is limited. Developing cost-effective integrated systems combining aromatic ring cleavage through processes like advanced oxidation (e.g., Fenton, ozonation, photocatalysis) is crucial [121,122]. Exploring conditions favoring high NM-ZVI reductive activity and simultaneous highly reactive oxidative species generation is essential for effective pollutant removal and detoxification.

(iv) The longevity of NM-ZVI requires further investigation. Practical application necessitates investigating NM-ZVI's long-term repeatability and exploring methods to enhance its structural integrity and durability [123]. Research should focus on novel approaches such as composites incorporation to protect NM-ZVI from corrosion and degradation [124,125], understanding underlying corrosion and aging mechanisms, and devising strategies to mitigate these issues for sustained remediation effectiveness.

CRediT authorship contribution statement

Zimin Yan: Investigation, Visualization, Writing - Original Draft. **Jia Ouyang:** Investigation, Writing - Review & Editing. **Bin Wu:** Supervision, Validation. **Chenchen Liu:** Data Curation, Software. **Hongcheng Wang:** Writing - Review & Editing. **Aijie Wang:** Writing - Review & Editing. **Zhiling Li:** Conceptualization, Methodology, Writing - Review & Editing.

Declaration of competing interest

The authors declare that they have no known competing financial interests or personal relationships that could have appeared to influence the work reported in this paper.

Acknowledgement

This research was supported by the NSFC-JSPS joint research program (No. 51961145202), the National Natural Science Foundation of China (No. 52370163, 52321005, and 52293443), and the State Key Laboratory of Urban Water Resource and Environment (Harbin Institute of Technology) (No. 2022TS42).

References

[1] D. Cao, X. Chen, J. Nan, A. Wang, Z. Li, Biomolecular insights into the inhibition of heavy metals on reductive dechlorination of 2,4,6-trichlorophenol in Pseudomonas sp. CP-1, Water Res. 247 (2023) 120836.
[2] L.M. Stevenson, A.S. Adeleye, Y. Su, Y. Zhang, A.A. Keller, R.M. Nisbet, Remediation of Cadmium toxicity by sulfidized nano-iron: the importance of organic material, ACS Nano 11 (2017) 10558–10567.
[3] M. Inyang, E. Dickenson, The potential role of biochar in the removal of organic and microbial contaminants from potable and reuse water: a review, Chemosphere 134 (2015) 232–240.
[4] F. He, L. Gong, D. Fan, P.G.G. Tratnyek, G.V.V. Lowry, Quantifying the efficiency and selectivity of organohalide dechlorination by zerovalent iron, Environ. Sci.:Processes Impacts 22 (2020) 528–542.
[5] Y. Wu, C.-Y. Guan, N. Griswold, L.-Y. Hou, X. Fang, A. Hu, Z.-Q. Hu, C.-P. Yu, Zero-valent iron-based technologies for removal of heavy metal(loid)s and organic pollutants from the aquatic environment: recent advances and perspectives, J. Clean. Prod. 277 (2020) 123478.
[6] S. Li, W. Wang, Y. Liu, W.X. Zhang, Zero-valent iron nanoparticles (nZVI) for the treatment of smelting wastewater: a pilot-scale demonstration, Chem. Eng. J. 254 (2014) 115–123.
[7] A. Galdames, L. Ruiz-Rubio, M. Orueta, M. Sanchez-Arzalluz, J. Luis Vilas-Vilela, Zero-valent iron nanoparticles for soil and groundwater remediation, Int. J. Environ. Res. Publ. Health 17 (2020) 5817.
[8] B.K. Khuntia, M.F. Anwar, T. Alam, M. Samim, M. Kumari, I. Arora, Synthesis and characterization of zero-valent iron nanoparticles, and the study of their effect against the degradation of DDT in soil and assessment of their toxicity against Collembola and ostracods, ACS Omega 4 (2019) 18502–18509.
[9] L.J. Matheson, P.G. Tratnyek, Reductive dehalogenation of chlorinated methanes by iron metal, Environ. Sci. Technol. 28 (1994) 2045–2053.
[10] J. Zhang, Z. Cheng, X. Yang, J. Luo, H. Li, H. Chen, Q. Zhang, J. Li, Mediating the reactivity and selectivity of nanoscale zerovalent iron toward nitrobenzene under porous carbon confinement, Chem. Eng. J. 393 (2020) 124779.
[11] S. Wang, Y. Song, Y. Sun, Enhanced dyes removal by sulfidated zerovalent iron: kinetics and influencing factors, Environ. Technol. Innov. 11 (2018) 339–347.
[12] J. Morales, R. Hutcheson, I.F. Cheng, Dechlorination of chlorinated phenols by catalyzed and uncatalyzed Fe^0 and Mg^0 particles, J. Hazard Mater. 90 (2002) 97–108.
[13] X. Guo, Z. Yang, H. Dong, X. Guan, Q. Ren, X. Lv, X. Jin, Simple combination of oxidants with zero-valent-iron (ZVI) achieved very rapid and highly efficient removal of heavy metals from water, Water Res. 88 (2016) 671–680.
[14] X. Guan, Y. Sun, H. Qin, J. Li, I.M.C. Lo, D. He, H. Dong, The limitations of applying zero-valent iron technology in contaminants sequestration and the corresponding countermeasures: the development in zero-valent iron technology in the last two decades (1994–2014), Water Res. 75 (2015) 224–248.
[15] J. Wang, J. Tang, Fe-based Fenton-like catalysts for water treatment: preparation, characterization and modification, Chemosphere 276 (2021) 130177.
[16] Z. Shi, D. Fan, R.L. Johnson, P.G. Tratnyek, J.T. Nurmi, Y. Wu, K.H. Williams, Methods for characterizing the fate and effects of nano zerovalent iron during groundwater remediation, J. Contam. Hydrol. 181 (2015) 17–35.
[17] A.S. Adeleye, L.M. Stevenson, Y. Su, R.M. Nisbet, Y. Zhang, A.A. Keller, Influence of phytoplankton on fate and effects of modified zerovalent iron nanoparticles, Environ. Sci. Technol. 50 (2016) 5597–5605.
[18] L. Ma, W.-X. Zhang, Enhanced biological treatment of industrial wastewater with bimetallic zero-valent iron, Environ. Sci. Technol. 42 (2008) 5384–5389.
[19] L. Liang, X. Guan, Z. Shi, J. Li, Y. Wu, P.G. Tratnyek, Coupled effects of aging and weak magnetic fields on sequestration of selenite by zero-valent iron, Environ. Sci. Technol. 48 (2014) 6326–6334.
[20] M. Stefaniuk, P. Oleszczuk, Y.S. Ok, Review on nano zerovalent iron (nZVI): from synthesis to environmental applications, Chem. Eng. J. 287 (2016) 618–632.
[21] B. Konadu-Amoah, R. Hu, A.I. Nde-Tchoupe, W. Gwenzi, C. Noubactep, Metallic iron (Fe^0)-based materials for aqueous phosphate removal: a critical review, J. Environ. Manag. 315 (2022) 115157.
[22] Y. Liu, S.A. Majetich, R.D. Tilton, D.S. Sholl, G.V. Lowry, TCE dechlorination rates, pathways, and efficiency of nanoscale iron particles with different properties, Environ. Sci. Technol. 39 (2005) 1338–1345.
[23] Y. Liu, T. Phenrat, G.V. Lowry, Effect of TCE concentration and dissolved groundwater solutes on NZVI-promoted TCE dechlorination and H_2 evolution, Environ. Sci. Technol. 41 (2007) 7881–7887.
[24] L. Gong, X. Qiu, D. Cheng, Y. Hu, Z. Zhang, Q. Yuan, D. Yang, C. Liu, L. Liang, F. He, Coincorporation of N and S into zero-valent iron to enhance TCE dechlorination: kinetics, electron efficiency, and dechlorination capacity, Environ. Sci. Technol. 55 (2021) 16088–16098.
[25] J. Xu, Z. Cao, H. Zhou, Z. Lou, Y. Wang, X. Xu, G.V. Lowry, Sulfur dose and sulfidation time affect reactivity and selectivity of post-sulfidized nanoscale zerovalent iron, Environ. Sci. Technol. 53 (2019) 13344–13352.
[26] Y. Gu, B. Wang, F. He, M.J. Bradley, P.G. Tratnyek, Mechanochemically sulfidated microscale zero valent iron: pathways, kinetics, mechanism, and efficiency of trichloroethylene dechlorination, Environ. Sci. Technol. 51 (2017) 12653–12662.
[27] S. Wang, M. Zhao, M. Zhou, Y.C. Li, J. Wang, B. Gao, S. Sato, K. Feng, W. Yin, A.D. Igalavithana, P. Oleszczuk, X. Wang, Y.S. Ok, Biochar-supported nZVI (nZVI/BC) for contaminant removal from soil and water: a critical review, J. Hazard Mater. 373 (2019) 820–834.
[28] R. Fu, X. Zhang, Z. Xu, X. Guo, D. Bi, W. Zhang, Fast and highly efficient removal of chromium (VI) using humus-supported nanoscale zero-valent iron: influencing factors, kinetics and mechanism, Sep. Purif. Technol. 174 (2017) 362–371.
[29] J. Xu, A. Avellan, H. Li, E.A. Clark, G. Henkelman, R. Kaegi, G.V. Lowry, Iron and sulfur precursors affect crystalline structure, speciation, and reactivity of sulfidized nanoscale zerovalent iron, Environ. Sci. Technol. 54 (2020) 13294–13303.
[30] J. Xu, Y. Wang, C. Weng, W. Bai, Y. Jiao, R. Kaegi, G.V. Lowry, Reactivity, selectivity, and long-term performance of sulfidized nanoscale zerovalent iron with different properties, Environ. Sci. Technol. 53 (2019) 5936–5945.
[31] S.R.C. Rajajayavel, S. Ghoshal, Enhanced reductive dechlorination of trichloroethylene by sulfidated nanoscale zerovalent iron, Water Res. 78 (2015) 144–153.
[32] Y. Han, W. Yan, Reductive dechlorination of trichloroethene by zero-valent iron nanoparticles: reactivity enhancement through sulfidation treatment, Environ. Sci. Technol. 50 (2016) 12992–13001.
[33] F. He, Z. Li, S. Shi, W. Xu, H. Sheng, Y. Gu, Y. Jiang, B. Xi, Dechlorination of excess trichloroethene by bimetallic and sulfidated nanoscale zero-valent iron, Environ. Sci. Technol. 52 (2018) 8627–8637.

[34] H. Li, Y.Q. Chen, S. Chen, X.L. Wang, S. Guo, Y.F. Qiu, Y.D. Liu, X.L. Duan, Y.J. Yu, Wheat straw biochar-supported nanoscale zerovalent iron for removal of trichloroethylene from groundwater, PLoS One 12 (2017) 0172337.
[35] J. Chen, H. Dong, R. Tian, R. Li, Q. Xie, Remediation of trichloroethylene-contaminated groundwater by sulfide-modified nanoscale zero-valent iron supported on biochar: investigation of critical factors, Water Air Soil Pollut. 231 (2020).
[36] Z. Cao, H. Li, G.V. Lowry, X. Shi, X. Pan, X. Xu, G. Henkelman, J. Xu, Unveiling the role of sulfur in rapid defluorination of florfenicol by sulfidized nanoscale zero-valent iron in water under ambient conditions, Environ. Sci. Technol. 55 (2021) 2628–2638.
[37] D. Li, Z. Mao, Y. Zhong, W. Huang, Y. Wu, P.a. Peng, Reductive transformation of tetrabromobisphenol A by sulfidated nano zerovalent iron, Water Res. 103 (2016) 1–9.
[38] Y. Ren, J. Ma, Y. Lee, Z. Han, M. Cui, B. Wang, M. Long, J. Khim, Reaction of activated carbon zerovalent iron with pentachlorophenol under anaerobic conditions, J. Clean. Prod. 297 (2021) 126748.
[39] J. Wan, X. Feng, Y. Li, J. He, N. Zhao, Z. Liu, Y. Lin, C. Yang, W. Liang, Effect of mesoporous silica molecular sieve coating on nZVI for 2,4-DCP degradation: morphology and mechanism during the reaction, Chem. Eng. Process Process Intensif. 135 (2019) 68–81.
[40] S. Song, Y. Su, A.S. Adeleye, Y. Zhang, X. Zhou, Optimal design and characterization of sulfide-modified nanoscale zerovalent iron for diclofenac removal, Appl. Catal. B Environ. 201 (2017) 211–220.
[41] M.B. Ahmed, J.L. Zhou, H.H. Ngo, W. Guo, M.A.H. Johir, K. Sornalingam, D. Belhaj, M. Kallel, Nano-Fe^0 immobilized onto functionalized biochar gaining excellent stability during sorption and reduction of chloramphenicol via transforming to reusable magnetic composite, Chem. Eng. J. 322 (2017) 571–581.
[42] X. Guan, X. Du, M. Liu, H. Qin, J. Qiao, Y. Sun, Enhanced trichloroethylene dechlorination by carbon-modified zero-valent iron: revisiting the role of carbon additives, J. Hazard Mater. 394 (2020) 122564.
[43] J. Gao, W. Wang, A.J. Rondinone, F. He, L. Liang, Degradation of trichloroethene with a novel ball milled Fe-C nanocomposite, J. Hazard Mater. 300 (2015) 443–450.
[44] F. Meng, J. Xu, H. Dai, Y. Yu, D. Lin, Even incorporation of nitrogen into Fe^0 nanoparticles as crystalline Fe_4N for efficient and selective trichloroethylene degradation, Environ. Sci. Technol. 56 (2022) 4489–4497.
[45] T. Li, X. Li, Y. Teng, H. Wang, H. Sun, Phosphidation of microscale zero-valent iron (P-mZVI) for enhanced dechlorination of trichloroethylene, J. Clean. Prod. 386 (2023) 135803.
[46] Y. Zhang, B. Yang, J. Fan, L. Ma, A mechanically synthesized SiO_2-Fe metal matrix composite for effective dechlorination of aqueous 2-chlorophenol: the optimum of the preparation conditions, RSC Adv. 6 (2016) 76867–76873.
[47] M. Brumovský, J. Oborná, V. Micić, O. Malina, J. Kašlík, D. Tunega, M. Kolos, T. Hofmann, F. Karlický, J. Filip, Iron nitride nanoparticles for enhanced reductive dechlorination of trichloroethylene, Environ. Sci. Technol. 56 (2022) 4425–4436.
[48] Y. Liu, S.P. Sohi, S. Liu, J. Guan, J. Zhou, J. Chen, Adsorption and reductive degradation of Cr(VI) and TCE by a simply synthesized zero valent iron magnetic biochar, J. Environ. Manag. 235 (2019) 276–281.
[49] H. Dong, C. Zhang, K. Hou, Y. Cheng, J. Deng, Z. Jiang, L. Tang, G. Zeng, Removal of trichloroethylene by biochar supported nanoscale zero-valent iron in aqueous solution, Sep. Purif. Technol. 188 (2017) 188–196.
[50] Y.-F. Su, Y.-L. Cheng, Y.-H. Shih, Removal of trichloroethylene by zerovalent iron/activated carbon derived from agricultural wastes, J. Environ. Manag. 129 (2013) 361–366.
[51] L. Wang, S.-Q. Ni, C. Guo, Y. Qian, One pot synthesis of ultrathin boron nitride nanosheet-supported nanoscale zerovalent iron for rapid debromination of polybrominated diphenyl ethers, J. Mater. Chem. A 1 (2013) 6379–6387.
[52] H. Chen, Y. Cao, E. Wei, T. Gong, Q. Xian, Facile synthesis of graphene nano zero-valent iron composites and their efficient removal of trichloronitromethane from drinking water, Chemosphere 146 (2016) 32–39.
[53] S.-Y. Oh, Y.-D. Seo, K.-S. Ryu, Reductive removal of 2,4-dinitrotoluene and 2,4-dichlorophenol with zero-valent iron-included biochar, Bioresour. Technol. 216 (2016) 1014–1021.
[54] X. Lv, J. Xu, G. Jiang, X. Xu, Removal of chromium(VI) from wastewater by nanoscale zero-valent iron particles supported on multiwalled carbon nanotubes, Chemosphere 85 (2011) 1204–1209.
[55] J. Han, G. Zhang, L. Zhou, F. Zhan, D. Cai, Z. Wu, Waste carton-derived nanocomposites for efficient removal of hexavalent chromium, Langmuir 34 (2018) 5955–5963.
[56] X. Li, L. Ai, J. Jiang, Nanoscale zerovalent iron decorated on graphene nanosheets for Cr(VI) removal from aqueous solution: surface corrosion retard induced the enhanced performance, Chem. Eng. J. 288 (2016) 789–797.
[57] Y. Li, T. Li, Z. Jin, Stabilization of Fe^0 nanoparticles with silica fume for enhanced transport and remediation of hexavalent chromium in water and soil, J. Environ. Sci. 23 (2011) 1211–1218.
[58] L. Qian, X. Shang, B. Zhang, W. Zhang, A. Su, Y. Chen, D. Ouyang, L. Han, J. Yan, M. Chen, Enhanced removal of Cr(VI) by silicon rich biochar-supported nanoscale zero-valent iron, Chemosphere 215 (2019) 739–745.
[59] Q. Zhang, Y. Wang, Z. Wang, Z. Zhang, X. Wang, Z. Yang, Active biochar support nano zero-valent iron for efficient removal of U(VI) from sewage water, J. Alloys Compd. 852 (2021) 156993.
[60] H. Pang, Z. Diao, X. Wang, Y. Ma, S. Yu, H. Zhu, Z. Chen, B. Hu, J. Chen, X. Wang, Adsorptive and reductive removal of U(VI) by Dictyophora indusiate-derived biochar supported sulfide NZVI from wastewater, Chem. Eng. J. 366 (2019) 368–377.
[61] M. Wu, X. Teng, X. Liang, Y. Zhang, Z. Huang, Y. Yin, Supporting nanoscale zero-valent iron onto shrimp shell-derived N-doped biochar to boost its reactivity and electron utilization for selenite sequestration, Chemosphere 319 (2023) 137979.
[62] S. Zhu, S.-H. Ho, X. Huang, D. Wang, F. Yang, L. Wang, C. Wang, X. Cao, F. Ma, Magnetic nanoscale zerovalent iron assisted biochar: interfacial chemical behaviors and heavy metals remediation performance, ACS Sustain. Chem. Eng. 5 (2017) 9673–9682.
[63] J. Li, X. Zhang, M. Liu, B. Pan, W. Zhang, Z. Shi, X. Guan, Enhanced reactivity and electron selectivity of sulfidated zerovalent iron toward chromate under aerobic conditions, Environ. Sci. Technol. 52 (2018) 2988–2997.
[64] W. Wang, B. Hu, C. Wang, Z. Liang, F. Cui, Z. Zhao, C. Yang, Cr(VI) removal by micron-scale iron-carbon composite induced by ball milling: the role of activated carbon, Chem. Eng. J. 389 (2020).
[65] K. Wang, Y. Sun, J. Tang, J. He, H. Sun, Aqueous Cr(VI) removal by a novel ball milled Fe0-biochar composite: role of biochar electron transfer capacity under high pyrolysis temperature, Chemosphere 241 (2020) 125044.
[66] K. Wei, H. Li, H. Gu, X. Liu, C. Ling, S. Cao, M. Li, M. Liao, X. Peng, Y. Shi, W. Shen, C. Liang, Z. Ai, L. Zhang, Strained zero-valent iron for highly efficient heavy metal removal, Adv. Funct. Mater. 32 (2022).
[67] Y. Yi, X. Wang, Y. Zhang, K. Yang, J. Ma, P. Ning, Formation and mechanism of nanoscale zerovalent iron supported by phosphoric acid modified biochar for highly efficient removal of Cr(VI), Adv. Powder Technol. 34 (2023) 103826.
[68] Y. Dai, Y. Hu, B. Jiang, J. Zou, G. Tian, H. Fu, Carbothermal synthesis of ordered mesoporous carbon-supported nano zero-valent iron with enhanced stability and activity for hexavalent chromium reduction, J. Hazard Mater. 309 (2016) 249–258.
[69] L.B. Hoch, E.J. Mack, B.W. Hydutsky, J.M. Hershman, J.M. Skluzacek, T.E. Mallouk, Carbothermal synthesis of carbon-supported nanoscale zero-valent iron particles for the remediation of hexavalent chromium, Environ. Sci. Technol. 42 (2008) 2600–2605.
[70] Z. Li, Y. Sun, Y. Yang, Y. Han, D.C.W. Tsang, Biochar-supported nanoscale zero-valent iron as an efficient catalyst for organic degradation in groundwater, J. Hazard Mater. 383 (2019) 121240.
[71] L. Liu, J. Zhao, X. Liu, S. Bai, H. Lin, D. Wang, Reduction and removal of As(V) in aqueous solution by biochar derived from nano zero-valent-iron (nZVI) and sewage sludge, Chemosphere 277 (2021) 130273.
[72] J. Xu, A. Avellan, H. Li, X. Liu, V. Noël, Z. Lou, Y. Wang, R. Kaegi, G. Henkelman, G.V. Lowry, Sulfur loading and speciation control the hydrophobicity, electron transfer, reactivity, and selectivity of sulfidized nanoscale zerovalent iron, Adv. Mater. 32 (2020) e1906910.
[73] J.-L. Do, T. Friscic, Mechanochemistry: a force of synthesis, ACS Cent. Sci. 3 (2017) 13–19.
[74] T. Friscic, C. Mottillo, H.M. Titi, Mechanochemistry for synthesis, Angew. Chem. Int. Ed. 59 (2020) 1018–1029.
[75] S.L. James, C.J. Adams, C. Bolm, D. Braga, P. Collier, T. Friscic, F. Grepioni, K.D.M. Harris, G. Hyett, W. Jones, A. Krebs, J. Mack, L. Maini, A.G. Orpen, I.P. Parkin, W.C. Shearouse, J.W. Steed, D.C. Waddell, Mechanochemistry: opportunities for new and cleaner synthesis, Chem. Soc. Rev. 41 (2012) 413–447.
[76] B.M. Rosen, V. Percec, Mechanochemistry - a reaction to stress, Nature 446 (2007) 381–382.
[77] W. Guo, Q. Zhao, J. Du, H. Wang, X. Li, N. Ren, Enhanced removal of sulfadiazine by sulfidated ZVI activated persulfate process: performance, mechanisms and degradation pathways, Chem. Eng. J. 388 (2020) 124303.
[78] W. Glasgow, B. Fellows, B. Qi, T. Darroudi, C. Kitchens, L. Ye, T.M. Crawford, O.T. Mefford, Continuous synthesis of iron oxide (Fe_3O_4) nanoparticles via thermal decomposition, Particuology 26 (2016) 47–53.
[79] X. Cao, H. Wang, C. Yang, L. Cheng, K. Fu, F. Qiu, Nanoscale zero-valent iron supported on carbon nanotubes for polychlorinated biphenyls removal. Desalin, Water Treat. 201 (2020) 173–186.
[80] Y. Yuan, N. Bolan, A. Prévoteau, M. Vithanage, J.K. Biswas, Y.S. Ok, H. Wang, Applications of biochar in redox-mediated reactions, Bioresour. Technol. 246 (2017) 271–281.
[81] X.-F. Tan, Y.-G. Liu, Y.-L. Gu, Y. Xu, G.-M. Zeng, X.-J. Hu, S.-B. Liu, X. Wang, S.-M. Liu, J. Li, Biochar-based nano-composites for the decontamination of wastewater: a review, Bioresour. Technol. 212 (2016) 318–333.
[82] S.-Y. Oh, Y.-D. Seo, K.-S. Ryu, D.-J. Park, S.-H. Lee, Redox and catalytic properties of biochar-coated zero-valent iron for the removal of nitro explosives and halogenated phenols, Environ. Sci.:Processes Impacts 19 (2017) 711–719.
[83] F. Yang, S. Zhang, Y. Sun, K. Cheng, J. Li, D.C.W. Tsang, Fabrication and characterization of hydrophilic corn stalk biochar-supported nanoscale zero-valent iron composites for efficient metal removal, Bioresour. Technol. 265 (2018) 490–497.
[84] Z. Tang, Z. Dai, M. Gong, H. Chen, X. Zhou, Y. Wang, C. Jiang, W. Yu, L. Li, Efficient removal of uranium(VI) from aqueous solution by a novel phosphate-modified biochar supporting zero-valent iron composite, Environ. Sci. Pollut. Res. 30 (2023) 40478–40489.
[85] J. Du, J. Bao, C. Lu, D. Werner, Reductive sequestration of chromate by hierarchical FeS@Fe^0 particles, Water Res. 102 (2016) 73–81.
[86] Y. Zhang, P. Ozcer, S. Ghoshal, A comprehensive assessment of the

degradation of C1 and C2 chlorinated hydrocarbons by sulfidated nanoscale zerovalent iron, Water Res. 201 (2021) 117328.
[87] E.-J. Kim, J.-H. Kim, A.-M. Azad, Y.-S. Chang, Facile synthesis and characterization of Fe/FeS nanoparticles for environmental applications, ACS Appl. Mater. Interfaces 3 (2011) 1457–1462.
[88] D. Fan, G. O'Brien Johnson, P.G. Tratnyek, R.L. Johnson, Sulfidation of nano zerovalent iron (nZVI) for improved selectivity during in-situ chemical reduction (ISCR), Environ. Sci. Technol. 50 (2016) 9558–9565.
[89] P. Fan, Y. Sun, B. Zhou, X. Guan, Coupled effect of sulfidation and ferrous dosing on selenate removal by zerovalent iron under aerobic conditions, Environ. Sci. Technol. 53 (2019) 14577–14585.
[90] G. Xu, H. Li, A.S.R. Bati, M. Bat-Erdene, M.J. Nine, D. Losic, Y. Chen, J.G. Shapter, M. Batmunkh, T. Ma, Nitrogen-doped phosphorene for electrocatalytic ammonia synthesis, J. Mater. Chem. A 8 (2020) 15875–15883.
[91] L. Gong, X. Qiu, P.G. Tratnyek, C. Liu, F. He, FeNX(C)-Coated microscale zerovalent iron for fast and stable trichloroethylene dechlorination in both acidic and basic pH conditions, Environ. Sci. Technol. 55 (2021) 5393–5402.
[92] P.-C. Shen, C. Su, Y. Lin, A.-S. Chou, C.-C. Cheng, J.-H. Park, M.-H. Chiu, A.-Y. Lu, H.-L. Tang, M.M. Tavakoli, G. Pitner, X. Ji, Z. Cai, N. Mao, J. Wang, V. Tung, J. Li, J. Bokor, A. Zettl, C.-I. Wu, T. Palacios, L.-J. Li, J. Kong, Ultralow contact resistance between semimetal and monolayer semiconductors, Nature 593 (2021) 211–217.
[93] B.Y. Zheng, H. Zhao, A. Manjavacas, M. McClain, P. Nordlander, N.J. Halas, Distinguishing between plasmon-induced and photoexcited carriers in a device geometry, Nat. Commun. 6 (2015) 7797.
[94] M. Li, Y. Mu, H. Shang, C. Mao, S. Cao, Z. Ai, L. Zhang, Phosphate modification enables high efficiency and electron selectivity of nZVI toward Cr(VI) removal, Appl. Catal. B Environ. 263 (2020) 118364.
[95] M. Li, H. Shang, H. Li, Y. Hong, C. Ling, K. Wei, B. Zhou, C. Mao, Z. Ai, L. Zhang, Kirkendall effect boosts phosphorylated nZVI for efficient heavy metal wastewater treatment, Angew. Chem. Int. Ed. 60 (2021) 17115–17122.
[96] Y. Zhang, B. Yang, Y. Han, C. Jiang, D. Wu, J. Fan, L. Ma, Novel iron metal matrix composite reinforced by quartz sand for the effective dechlorination of aqueous 2-chlorophenol, Chemosphere 146 (2016) 308–314.
[97] Y.J. Oh, H. Song, W.S. Shin, S.J. Choi, Y.-H. Kim, Effect of amorphous silica and silica sand on removal of chromium(VI) by zero-valent iron, Chemosphere 66 (2007) 858–865.
[98] X. Kong, Z. Han, W. Zhang, L. Song, H. Li, Synthesis of zeolite-supported microscale zero-valent iron for the removal of Cr^{6+} and Cd^{2+} from aqueous solution, J. Environ. Manag. 169 (2016) 84–90.
[99] E. Salama, M. Samy, H. Shokry, G. El-Subruiti, A. El-Sharkawy, H. Hamad, M. Elkady, The superior performance of silica gel supported nano zero-valent iron for simultaneous removal of Cr (VI), Sci. Rep. 12 (2022) 22443.
[100] D. Fan, R.P. Anitori, B.M. Tebo, P.G. Tratnyek, J.S. Lezama Pacheco, R.K. Kukkadapu, M.H. Engelhard, M.E. Bowden, L. Kovarik, B.W. Arey, Reductive sequestration of pertechnetate ($^{99}TcO_4^-$) by nano zerovalent iron (nZVI) transformed by abiotic sulfide, Environ. Sci. Technol. 47 (2013) 5302–5310.
[101] E.-J. Kim, K. Murugesan, J.-H. Kim, P.G. Tratnyek, Y.-S. Chang, Remediation of trichloroethylene by FeS-coated iron nanoparticles in simulated and real groundwater: effects of water chemistry, Ind. Eng. Chem. Res. 52 (2013) 9343–9350.
[102] Y. Gong, L. Gai, J. Tang, J. Fu, Q. Wang, E.Y. Zeng, Reduction of Cr(VI) in simulated groundwater by FeS-coated iron magnetic nanoparticles, Sci. Total Environ. 595 (2017) 743–751.
[103] Y. Su, A.S. Adeleye, A.A. Keller, Y. Huang, C. Dai, X. Zhou, Y. Zhang, Magnetic sulfide-modified nanoscale zerovalent iron (S-nZVI) for dissolved metal ion removal, Water Res. 74 (2015) 47–57.
[104] N. Zhou, K. Gong, Q. Hu, X. Cheng, J. Zhou, M. Dong, N. Wang, T. Ding, B. Qiu, Z. Guo, Optimizing nanocarbon shell in zero-valent iron nanoparticles for improved electron utilization in Cr(VI) reduction, Chemosphere 242 (2020) 125235.
[105] M.M. Scherer, B.A. Balko, P.G. Tratnyek, The role of oxides in reduction reactions at the metal-water interface, ACS 715 (1999) 301–322.
[106] B. Hammer, J.K. Norskov, Why gold is the noblest of all the metals, Nature 376 (1995) 238–240.
[107] J. Xu, H. Li, G.V. Lowry, Sulfidized nanoscale zero-valent iron: tuning the properties of this complex material for efficient groundwater remediation, Acc. Mater. Res. 2 (2021) 420–431.
[108] F. Gao, H. Lyu, S. Ahmad, S. Xu, J. Tang, Enhanced reductive degradation of tetrabromobisphenol A by biochar supported sulfidated nanoscale zero-valent iron: selectivity and core reactivity, Appl. Catal. B Environ. 324 (2023) 122246.
[109] Y. Mu, F. Jia, Z. Ai, L. Zhang, Iron oxide shell mediated environmental remediation properties of nano zero-valent iron, Environ. Sci.: Nano 4 (2017) 27–45.
[110] C. Noubactep, A critical review on the process of contaminant removal in Fe^0-H_2O systems, Environ. Technol. 29 (2008) 909–920.
[111] H. Qin, J. Li, H. Yang, B. Pan, W. Zhang, X. Guan, Coupled effect of ferrous ion and oxygen on the electron selectivity of zerovalent iron for selenate sequestration, Environ. Sci. Technol. 51 (2017) 5090–5097.
[112] H. Liu, Q. Wang, C. Wang, X.Z. Li, Electron efficiency of zero-valent iron for groundwater remediation and wastewater treatment, Chem. Eng. J. 215 (2013) 90–95.
[113] P. Schoeftner, G. Waldner, W. Lottermoser, M. Stoeger-Pollach, P. Freitag, T.G. Reichenauer, Electron efficiency of nZVI does not change with variation of environmental parameters, Sci. Total Environ. 535 (2015) 69–78.
[114] M. Keiluweit, P.S. Nico, M.G. Johnson, M. Kleber, Dynamic molecular structure of plant biomass-derived black carbon (biochar), Environ. Sci. Technol. 44 (2010) 1247–1253.
[115] B. Chen, D. Zhou, L. Zhu, Transitional adsorption and partition of nonpolar and polar aromatic contaminants by biochars of pine needles with different pyrolytic temperatures, Environ. Sci. Technol. 42 (2008) 5137–5143.
[116] X. Hu, Z. Ding, A.R. Zimmerman, S. Wang, B. Gao, Batch and column sorption of arsenic onto iron-impregnated biochar synthesized through hydrolysis, Water Res. 68 (2015) 206–216.
[117] P. Fan, X. Zhang, H. Deng, X. Guan, Enhanced reduction of p-nitrophenol by zerovalent iron modified with carbon quantum dots, Appl. Catal. B Environ. 285 (2021) 119829.
[118] H. Li, W. Yang, C. Wu, J. Xu, Origin of the hydrophobicity of sulfur-containing iron surfaces, Phys. Chem. Chem. Phys. 23 (2021) 13971–13976.
[119] J. Zhang, X. Zhao, W. Wang, Z. Song, Y. Mao, J. Sun, S. Chen, Removal of p-nitrophenol by double-modified nanoscale zero-valent iron with biochar and sulfide: Key factors and mechanisms, J. Water Process Eng. 51 (2023) 103398.
[120] Z. Zhang, Z. Li, X. Chen, J. Nan, Y. Zu, F. Chen, B. Liang, A. Wang, Molecular insights into the response of nonelectroactive bacteria to electrostimulation: growth and metabolism regulation mechanism, ACS ES&T Engineering (2024), https://doi.org/10.1021/acsestengg.3c00472.
[121] W. Xu, J. Zhang, T. Xu, X. Hu, C. Shen, L. Lou, Could sulfidation enhance the long-term performance of nano-zero valent iron in the peroxymonosulfate activation to degrade 2-chlorobiphenyl? Environ. Pollut. 316 (2023) 120631.
[122] B. Wu, Z. Li, Y. Zu, B. Lai, A. Wang, Polar electric field-modulated peroxymonosulfate selective activation for removal of organic contaminants via non-radical electron transfer process, Water Res. 246 (2023) 120678.
[123] M. Vogel, A. Georgi, F.-D. Kopinke, K. Mackenzie, Sulfidation of ZVI/AC composite leads to highly corrosion-resistant nanoremediation particles with extended life-time, Sci. Total Environ. 665 (2019) 235–245.
[124] B. Sahu, P. Sinha, D. Kumar, K. Patel, S. Banerjee, Magnetically recyclable nanoscale zero-valent iron-mediated PhotoRDRP in ionic liquid toward smart, functional polymers, Macromol. Rapid Commun. (2023), https://doi.org/10.1002/marc.202300500, 2023.
[125] D. Kumar, B. Sahu, S. Dolui, S.S. Rajput, M.M. Alam, S. Banerjee, Multi-stimuli responsive boronic acid-containing polymers via recyclable nanoscale zerovalent iron (nZVI)-mediated photoRDRP in ionic liquid, Eur. Polym. J. 199 (2023) 112443.